

Effect of Sodium Fluoride on the Stability of Dental Alloys in Artificial Saliva

DANIELA COVACIU ROMONT¹, INGRID MILOSEV², IOANA DEMETRESCU^{1*}

¹University Politehnica of Bucharest, Faculty of Applied Chemistry and Materials Science, 1-7 Polizu Str., 011061, Bucharest, Romania

²Jozef Stefan Institute, Department of Physical and Organic Chemistry, Jamova 39, SI-6280, Slovenia

Dental alloys as CoCrMo, SS 316L stainless steel and NiTi were electrochemically investigated in artificial Fusayama saliva, unmodified and modified with two different concentrations of sodium fluoride. Electrochemical tests include measurements of open circuit, measurements of linear polarization, potentiodynamic polarization curves and electrochemical impedance spectra. The best electrochemical behavior with a good corrosion resistance was found for the CoCrMo alloy, followed by stainless steel alloy. NiTi alloy was the most affected by the addition of fluoride and the corrosion rate decreased dramatically. Based on our experimental data we can conclude that the addition of sodium fluoride increases the corrosion rate.

Keywords: dental alloys, electrochemical stability, artificial saliva, sodium fluoride

Titanium and titanium alloys [1], CoCrMo [2,3] and stainless steel alloys [4] are extensively used for dental restoration in oral cavity [5] being selected for their good physical properties [6]. Despite the fact that Ni is considered an allergen nickel-titanium alloys are used as well having remarkable properties [7] due to the formation of TiO₂ on its the surface. So called memory alloys containing nickel can be manufactured using new technologies and producing new generation of implants with a porous microstructure very similar to the human bone [8]. At the beginning of the last century, CoCrMo alloys were used in dental and orthopaedic applications due to their very good mechanical properties, corrosion and wear resistance. The corrosion resistance of CoCrMo alloys in different aggressive environments is related to the formation of oxide films of CoO and Cr₂O₃ [9]. The addition of molybdenum in this alloy improves the mechanical properties. Being not expensive, medical stainless steel alloys are also used in dentistry for their good corrosion resistance in bio liquids. The chemical composition of biomedical stainless steel alloy indicates high percentage of chromium and nickel which improves corrosion properties. Of course, the low price is not the only advantage for the use of these materials, but the biocompatibility, the mechanical properties and good electrochemical behavior are factors which sustain the use of these materials in dental and orthopaedic medicine.

Regarding NiTi alloy, known as nitinol, its passivity is due to TiO₂ film formed at surface according to the fact that oxidation of Ti is thermodynamically more favorable process than that of Ni [10]. Low nickel content in the oxide layer, which can be explained by the various values of free energy formation for these two oxides, is important for its biocompatibility, as titanium itself having no harmful effects. For longer period of time in oral cavity, Ni²⁺ ions release as a corrosion effect could be dangerous taking into account its allergenic action [11,12]. The kinetic aspects of NiTi passivity for unmodified and thermally treated samples was investigated intensively [13,14], and the barrier properties of oxide films were established [12]. Fluoride which is present in oral hygiene products such as

tooth paste or mouthwashes for caries prevention has merits and demerits actions, as reported for Ti alloys [15], and there is a need for more investigations. The addition of fluoride [16] in small amounts (5000 ppm) promotes remineralization of teeth and is preventing tooth decay. Too much fluoride can cause mottling of the teeth - meaning fluorosis [17]. The fluoride effect on various alloys is not completely understood [18]. Taking into account the complex role of fluoride, the aim of the present paper is to study the behavior of dental alloys in artificial saliva with and without addition of different amounts of fluoride.

Experimental part

Samples preparation

Samples of CoCrMo (26-30% Cr, 5-7% Mo and Co in balance), SS 316L (16-18% Cr, 10-14% Ni, 2-3% Mo, 2% Mn and Fe in balance) and NiTi (54.5% Ni and Ti in balance) alloys, with dimensions of 15 mm in diameter and 2 mm thick, were electrochemically investigated in artificial saliva, Fusayama [19] and modified Fusayama. The metallic samples were wet grinding with abrasive SiC paper from 320 to 4000 grits (Struers, Ballerup, Denmark). After polishing samples were cleaned in ethylic alcohol in an ultrasound bath for 5 min. In the end the cleaned samples were rinsed with double distilled water and dried in a flow of nitrogen.

Preparation of artificial modified and unmodified Fusayama saliva

The used electrolyte (E1, E2 and E3) solutions were artificial saliva and modified artificial saliva with 0.1% and 0.25% of sodium fluoride. The chemical composition of the electrolytes is presented in table 1. Chemicals were provided by Sigma Aldrich.

Electrochemical measurements

Electrochemical tests include measurements of open circuit potential (E_{oc}), for a period of 1 h, measurements of linear polarization, potentiodynamic polarization curves and electrochemical impedance spectra. Polarization resistance (R_p) was determined from linear polarization

* email: ioana_demetrescu@yahoo.com

Table 1
CHEMICAL COMPOSITION OF ARTIFICIAL SALIVA FUSAYAMA (E1)
AND MODIFIED FUSAYAMA (E2 and E3)

Compound (g/L)	E1	E2	E3
NaCl	0.4	0.4	0.4
KCl	0.4	0.4	0.4
CaCl ₂ ·2H ₂ O	0.795	0.795	0.795
NaH ₂ PO ₄ ·2H ₂ O	0.78	0.78	0.78
H ₂ O			
Na ₂ S·9 H ₂ O	0.005	0.005	0.005
Urea	1	1	1
NaF	-	1	2.5

(LP) using $[-0.01 \div 0.01 \text{ V}]$ for start and stop potential and a scan rate of 0.0001 V/s . Electrochemical parameters as corrosion potential (E_{corr}) and corrosion current density (j_{corr}) were determined measuring potentiodynamic polarization curves with a start potential -0.25 V and a stop potential between 1.0 and 1.5 V . The scan rate was 0.001 V/s . Electrochemical impedance spectroscopy (EIS) measurements were carried out with start frequency 100 kHz and finish frequency 5 mHz with an amplitude of 10 mV . EIS parameters like solution resistance (R_s), polarization resistance (R_p), constant phase element (CPE) were calculated using EIS Spectrum analyzer. The experimental data were processed using SigmaPlot Software, Version 11.0.

Electrochemical measurements were carried out using a Potentiostat Parstat 2263, Princeton Applied Research. The system used for electrochemical determinations was a three electrode cell with a reference electrode Ag/AgCl (3M), working electrode as CoCrMo, SS 316L and NiTi samples and stainless steel as a counterelectrode. The metallic samples were inserted into a Teflon holder and the exposed surface to the electrolyte solution was 0.785 cm^2 .

Surface analysis by profilometry

The topography of the samples before and after immersion in artificial saliva Fusayama and modified Fusayama for 240 h was measured using profilometer Dektat XT Bruker Nano Surfaces Division Stylus Profiler equipped with Vision 64 Version 5.40 Update 6 Software.

All the images were processed with Taly Map Gold, Version 6.2.6.746 Software.

Results and discussions

Electrochemical measurements

Measurements of open-circuit potential (E_{oc}) were performed for 1 hour for each alloy in all environments mentioned above. Figure 1 presents the OCP curves recorded for CoCrMo alloys, 316L SS and NiTi. It can be noticed that the variation of the potential in Fusayama solution presents a shift tendency to more electropositive potential values for SS 316L and NiTi alloys. For CoCrMo the steady state is not reached, fact that proves the ability of the alloy to continuously auto-passivate.

The addition of fluoride in artificial saliva influence only the electrochemical behavior of NiTi alloy, shifting the potential to more negative values compared to the initial value. CoCrMo and SS316L in modified Fusayama present similar behavior but without steady state at the end of the experiment.

In order to measure the corrosion parameters, potentiodynamic polarization curves were measured (fig. 2).

The shape of the potentiodynamic polarization curves indicates a different extent of passivity range for each alloy. The electrochemical behaviour of CoCrMo shows a larger passive interval compared with SS 316L. It is important to mention that all alloys present passivity in a positive domain. Corrosion parameters are presented in tables 2, 3 and 4. The smallest values for corrosion current density were recorded for CoCrMo alloy, followed by SS 316L and NiTi.

The highest values of polarization resistance are correlated with the smallest corrosion current densities. It can be observed that the best electrochemical parameters were recorded in case of Fusayama solution. According to the experimental data it is to mention that the addition of sodium fluoride increases corrosion rate and decreases the polarization resistance relative to the amount of fluoride added.

The electrochemical impedance spectroscopy tests were performed for each alloy, separately for a period of 240 h . In figure 3 are presented fitted EIS diagrams for CoCrMo in all electrolytes.

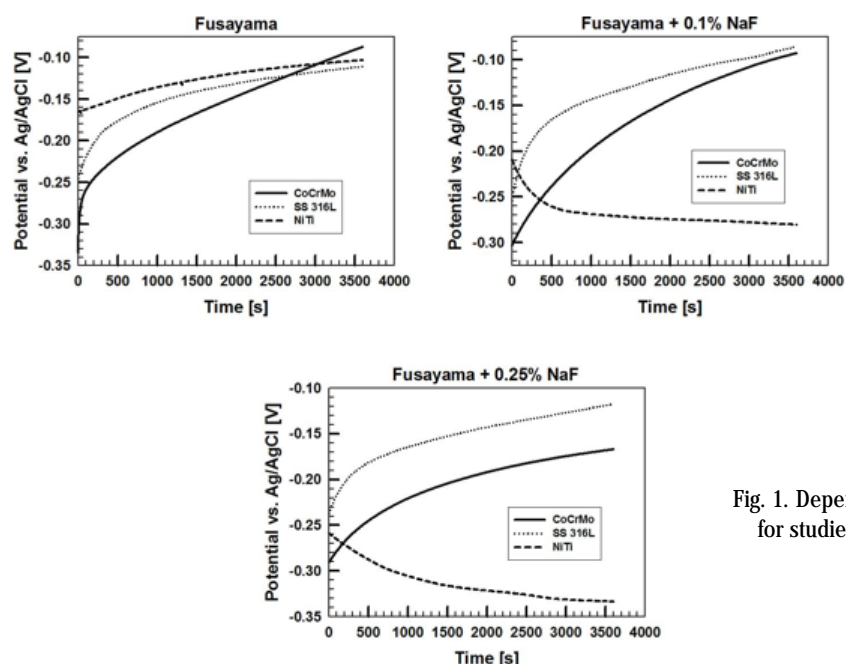


Fig. 1. Dependence on open circuit potential (E_{oc}) with time for studied alloys in Fusayama and modified Fusayama

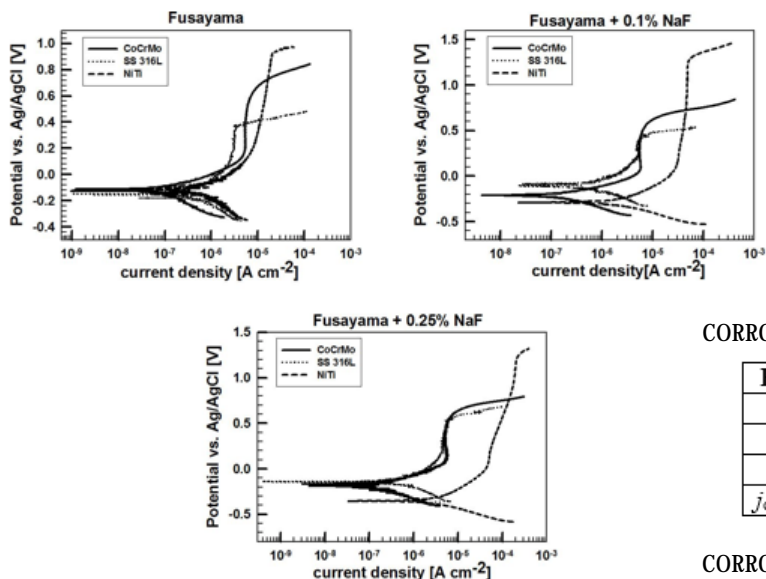


Fig. 2. Potentiodynamic polarization curves for CoCrMo, SS 316L and NiTi in Fusayama (E1), Fusayama with 0.1% NaF (E2) and Fusayama with 0.25% NaF (E3)

Table 2

CORROSION PARAMETERS FOR CoCrMo, SS 316L AND NiTi IN E1

Parameter*	CoCrMo	SS 316L	NiTi
E_{oc} [mV]	-87	-111	-103
R_p [Ωcm^2]	$8.1 \cdot 10^5$	$7.0 \cdot 10^5$	$2.3 \cdot 10^5$
E_{corr} [mV]	-144	-159	-134
j_{corr} [$\mu\text{A}/\text{cm}^2$]	$1.08 \cdot 10^{-2}$	$2.56 \cdot 10^{-2}$	$6.43 \cdot 10^{-2}$

Table 3

CORROSION PARAMETERS FOR CoCrMo, SS 316L AND NiTi IN E2

Parameter*	CoCrMo	SS 316L	NiTi
E_{oc} [mV]	-93	-85	-280
R_p [Ωcm^2]	$4.1 \cdot 10^5$	$1.7 \cdot 10^5$	$2.5 \cdot 10^4$
E_{corr} [mV]	-151	-99	-318
j_{corr} [$\mu\text{A}/\text{cm}^2$]	$1.34 \cdot 10^{-2}$	$4.74 \cdot 10^{-2}$	2.74

Table 4

CORROSION PARAMETERS FOR CoCrMo, SS 316L AND NiTi IN E3

Parameter*	CoCrMo	SS 316L	NiTi
E_{oc} [mV]	-167	-118	-333
R_p [Ωcm^2]	$3.1 \cdot 10^5$	$3.3 \cdot 10^5$	$1.9 \cdot 10^4$
E_{corr} [mV]	-189	-128	-375
j_{corr} [$\mu\text{A}/\text{cm}^2$]	$1.54 \cdot 10^{-2}$	$3.60 \cdot 10^{-2}$	2.90

* E_{oc} - open circuit potential; E_{corr} - corrosion potential; j_{corr} - corrosion current density; R_p - polarization resistance

According to EIS measurements a constant increase of polarization resistance in time can be observed. Equivalent electrical circuit (EEC) used is shown in figure 4.

High impedances in order of $10^5 \Omega$ were obtained at low and medium frequencies suggesting good corrosion resistance of CoCrMo alloy. The phase angles of -80 to -90 degrees at medium frequencies suggests the formation of a compact passive film at the interface.

Mathematical modeling of the process was done by establishing and interpreting an electrical equivalent circuit for best fitting of Nyquist diagrams (fig. 4a). In this circuit R1 is the equivalent ohmic resistance of the electrolyte and R2 - CPE1 (sub-circuit) is the ohmic resistance of passive film on the surface of the alloy and characteristic of double-layer capacitive electrical interface biomaterial / solution. Fitted parameters are presented in table 5.

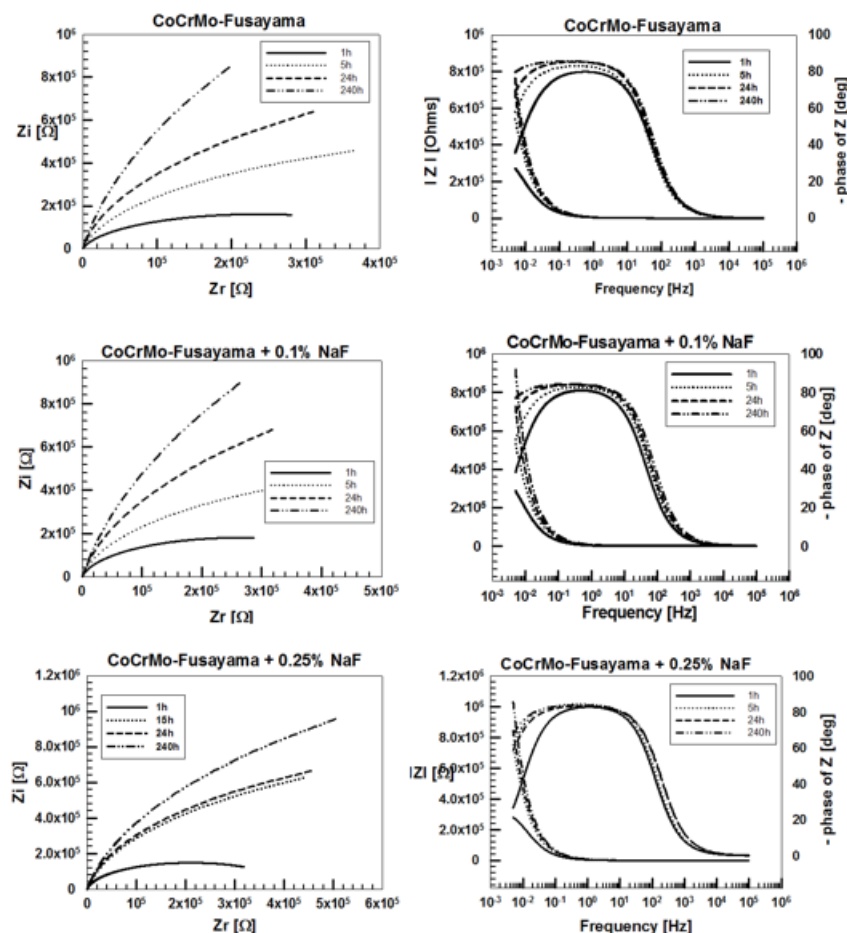


Fig. 3. Fitted EIS diagrams for CoCrMo in Fusayama (E1), Fusayama with 0.1% NaF (E2) and Fusayama with 0.25% NaF (E3) up to 240 h

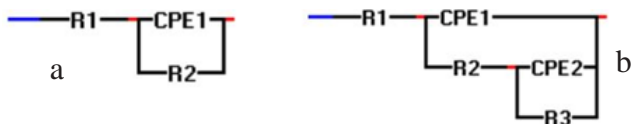


Fig. 4. Electrical equivalent circuit used for fitting electrochemical data

Electrolyte	t [h]	R_s [Ωcm^2]	R_p [Ωcm^2]	CPE	n
E1	1	$1.32 \cdot 10^2$	$4.75 \cdot 10^5$	$3.94 \cdot 10^{-5}$	0.90
	5	$1.61 \cdot 10^2$	$1.63 \cdot 10^6$	$3.15 \cdot 10^{-5}$	0.93
	24	$1.33 \cdot 10^2$	$2.99 \cdot 10^6$	$2.93 \cdot 10^{-5}$	0.96
	240	$1.41 \cdot 10^2$	$9.88 \cdot 10^6$	$2.45 \cdot 10^{-5}$	0.95
E2	1	$1.34 \cdot 10^2$	$5.21 \cdot 10^5$	$4.11 \cdot 10^{-5}$	0.92
	5	$1.35 \cdot 10^2$	$1.41 \cdot 10^6$	$3.06 \cdot 10^{-5}$	0.93
	24	$1.32 \cdot 10^2$	$3.61 \cdot 10^6$	$2.63 \cdot 10^{-5}$	0.94
	240	$1.33 \cdot 10^2$	$3.83 \cdot 10^6$	$2.16 \cdot 10^{-5}$	0.94
E3	1	$0.59 \cdot 10^2$	$4.19 \cdot 10^5$	$3.22 \cdot 10^{-5}$	0.93
	5	$0.62 \cdot 10^2$	$2.31 \cdot 10^6$	$2.42 \cdot 10^{-5}$	0.93
	24	$0.66 \cdot 10^2$	$2.42 \cdot 10^6$	$2.41 \cdot 10^{-5}$	0.94
	240	$0.69 \cdot 10^2$	$4.56 \cdot 10^6$	$1.79 \cdot 10^{-5}$	0.93

Table 5
EIS PARAMETERS FOR CoCrMo IN FUSAYAMA (E1), FUSAYAMA WITH 0.1% NaF (E2) AND FUSAYAMA WITH 0.25% NaF (E3) UP TO 240 h

Electrochemical impedance measurements for SS 316L in artificial modified and unmodified saliva are presented in figure 5. The results obtained in the artificial saliva Fusayama SS 316L are fitted with the EEC in figure 4a. Similar behavior is observed. Results obtained in saliva solution containing 0.1% NaF were fitted using the EEC in figure 4b.

Bode diagrams shown in figure 5. are similar in all cases, characterized by two distinct regions. In the region of higher frequency (1-10 kHz), Bode diagrams have constant values of the $|Z|$ vs. $\log(f)$. This is due to the response resistance of the electrolyte. In the domain of low and medium frequencies, spectrum displays a linear slope about -1. This is a characteristic response of the film surface capacitive behaviour.

The electrochemical parameters of EIS determination for SS 316L in all electrolytes are presented in table 6.

Fitted EIS diagrams from NiTi alloys measurements are shown in figure 6. The polarization resistance is increasing with time. The electrical equivalent circuit used for fitting the electrochemical data is shown in figure 4a.

Phase angle decreases significantly, to small values in the lower region of frequencies, which demonstrates that the impedance acts as a pure resistance of the film surface. However, the phase angle is close to -80° maintained in a wide range of frequencies, indicating an almost capacitive response of all the materials studied. This behavior indicates the presence of a thin passive oxide film on the surface of materials.

In table 7 are presented the EIS parameters for alloy NiTi. Analyzing the electrochemical data, it can be observed a increasing of R_p and a decreasing of CPE, respectively. Comparing the environments it is to mention that polarization resistance decreases with the addition of NaF.

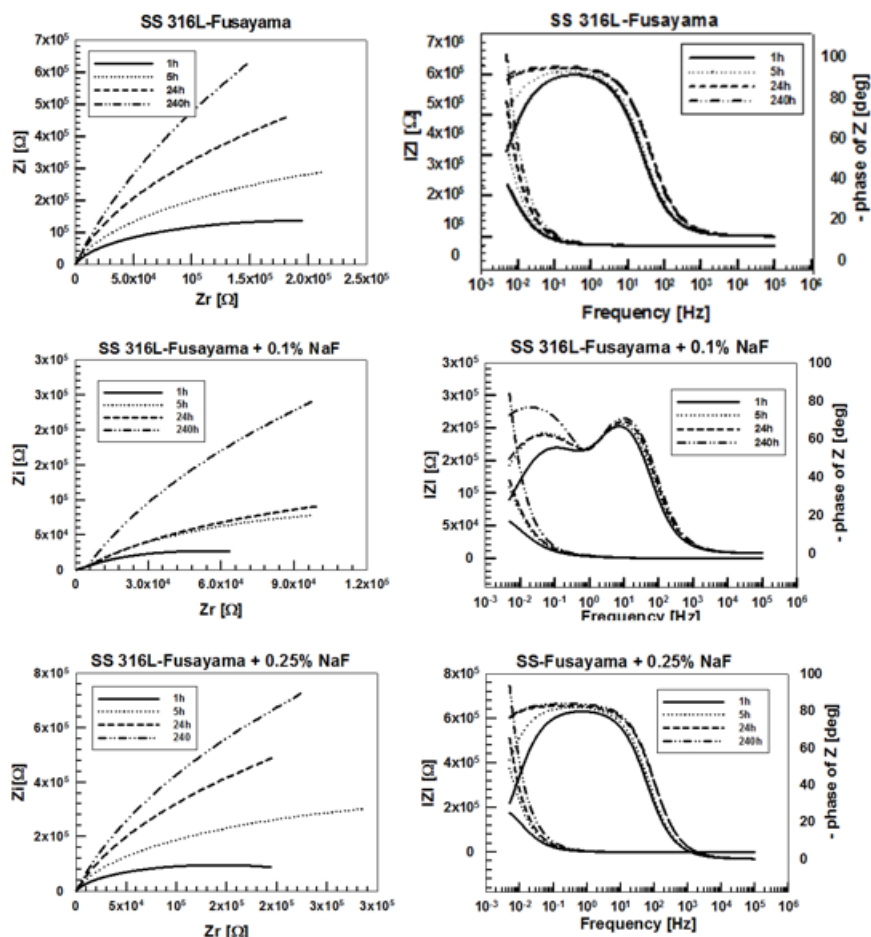


Fig. 5. Fitted EIS diagrams for SS 316L in Fusayama (E1), Fusayama with 0.1% NaF (E2) and Fusayama with 0.25% NaF (E3) up to 240 h

Electrolyte	t [h]	R_s [Ωcm^2]	R_{p1} [Ωcm^2]	R_{p2} [Ωcm^2]	CPE1	CPE2	$n1$	$n2$
E1	1	$1.68 \cdot 10^2$	$4.01 \cdot 10^5$	-	$5.99 \cdot 10^{-5}$	-	0.91	-
	5	$1.75 \cdot 10^2$	$1.10 \cdot 10^6$	-	$4.99 \cdot 10^{-5}$	-	0.92	-
	24	$1.76 \cdot 10^2$	$3.08 \cdot 10^6$	-	$3.99 \cdot 10^{-5}$	-	0.93	-
	240	$1.79 \cdot 10^2$	$9.91 \cdot 10^6$	-	$3.11 \cdot 10^{-5}$	-	0.93	-
E2	1	$1.30 \cdot 10^2$	$4.83 \cdot 10^3$	$9.92 \cdot 10^4$	$3.21 \cdot 10^{-5}$	$8.35 \cdot 10^{-5}$	0.93	0.74
	5	$1.33 \cdot 10^2$	$5.29 \cdot 10^3$	$2.98 \cdot 10^5$	$2.60 \cdot 10^{-5}$	$6.91 \cdot 10^{-5}$	0.94	0.77
	24	$1.31 \cdot 10^2$	$5.43 \cdot 10^3$	$4.23 \cdot 10^5$	$2.18 \cdot 10^{-5}$	$6.30 \cdot 10^{-5}$	0.95	0.75
	240	$1.31 \cdot 10^2$	$7.71 \cdot 10^3$	$2.22 \cdot 10^6$	$1.99 \cdot 10^{-5}$	$4.95 \cdot 10^{-5}$	0.94	0.89
E3	1	$8.62 \cdot 10^2$	$2.83 \cdot 10^5$	-	$5.21 \cdot 10^{-5}$	-	0.91	-
	5	$8.89 \cdot 10^2$	$9.66 \cdot 10^5$	-	$4.10 \cdot 10^{-5}$	-	0.92	-
	24	$9.11 \cdot 10^2$	$3.57 \cdot 10^6$	-	$3.59 \cdot 10^{-5}$	-	0.92	-
	240	$9.2 \cdot 10^2$	$7.05 \cdot 10^6$	-	$2.40 \cdot 10^{-5}$	-	0.93	-

Table 6
EIS PARAMETERS FOR SS 316L IN FUSAYAMA (E1), FUSAYAMA WITH 0.1% NaF (E2) AND FUSAYAMA WITH 0.25% NaF (E3) UP TO 240 h

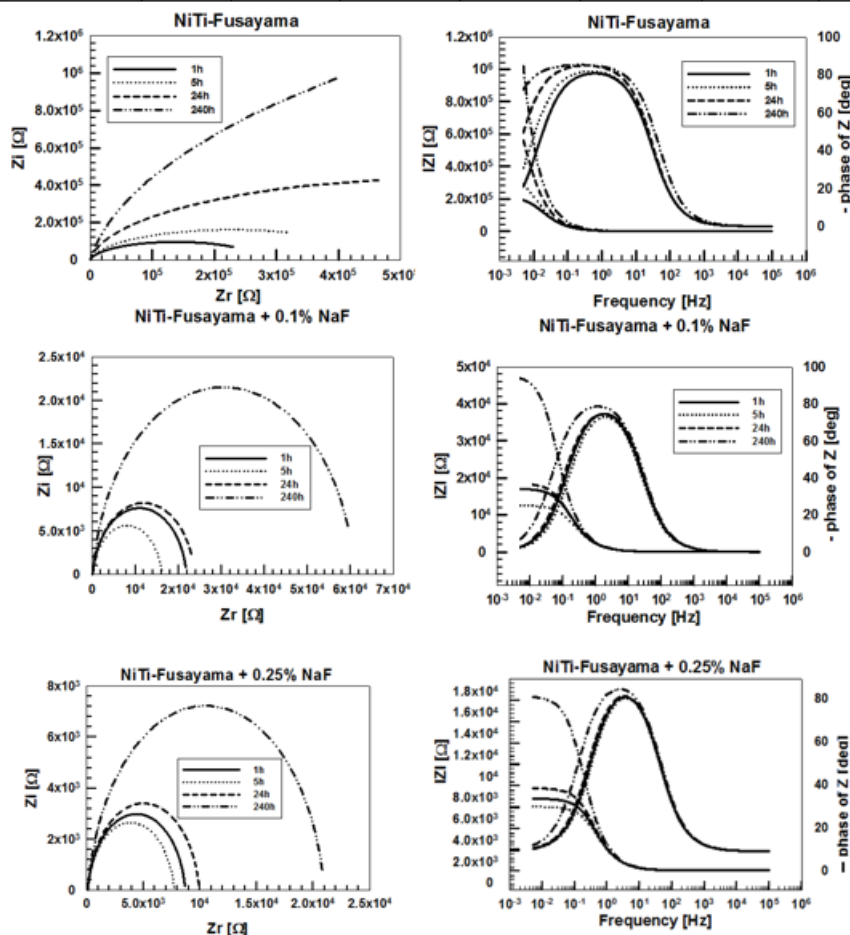


Fig. 6. Fitted EIS diagrams for NiTi in Fusayama (E1), Fusayama with 0.1% NaF (E2) and Fusayama with 0.25% NaF (E3) up to 240 h

Electrolyte	t [h]	R_s [Ωcm^2]	R_p [Ωcm^2]	CPE	n
E1	1	$2.06 \cdot 10^2$	$2.76 \cdot 10^5$	$3.66 \cdot 10^{-5}$	0.93
	5	$2.06 \cdot 10^2$	$4.57 \cdot 10^5$	$3.56 \cdot 10^{-5}$	0.94
	24	$2.15 \cdot 10^2$	$1.19 \cdot 10^6$	$2.93 \cdot 10^{-5}$	0.96
	240	$2.16 \cdot 10^2$	$5.51 \cdot 10^6$	$1.99 \cdot 10^{-5}$	0.95
E2	1	$1.45 \cdot 10^2$	$2.17 \cdot 10^4$	$5.65 \cdot 10^{-5}$	0.93
	5	$1.48 \cdot 10^2$	$1.60 \cdot 10^4$	$6.25 \cdot 10^{-5}$	0.93
	24	$1.47 \cdot 10^2$	$2.36 \cdot 10^4$	$5.50 \cdot 10^{-5}$	0.92
	240	$1.47 \cdot 10^2$	$6.08 \cdot 10^4$	$5.11 \cdot 10^{-5}$	0.93
E3	1	$0.91 \cdot 10^2$	$8.60 \cdot 10^3$	$6.43 \cdot 10^{-5}$	0.92
	5	$0.90 \cdot 10^2$	$7.62 \cdot 10^3$	$6.57 \cdot 10^{-5}$	0.92
	24	$0.91 \cdot 10^2$	$9.84 \cdot 10^3$	$6.30 \cdot 10^{-5}$	0.92
	240	$0.94 \cdot 10^2$	$2.08 \cdot 10^4$	$5.79 \cdot 10^{-5}$	0.92

Table 7
EIS PARAMETERS FOR NiTi IN FUSAYAMA (E1), FUSAYAMA WITH 0.1% NaF (E2) AND FUSAYAMA WITH 0.25% NaF (E3) UP TO 240 h

According to experimental data, in all cases it can be notice that polarisation resistance increases in time.

For the evaluation of the roughness surface of the metallic samples saliva a topographic analysis was carried out. After immersion in artificial saliva with and without NaF for 10 days the surface of CoCrMo, SS 316L and NiTi alloys was examined. 3D images of the topography of

reference alloys and after immersion are presented in figures 7-9. Figures present the coloration according to the scale (1.25-1.5 μm) placed in the right side of the figure.

The roughness values are presented in Table 8. CoCrMo alloys present the highest values of roughness in Fusayama and modified Fusayama compared to the reference alloy.

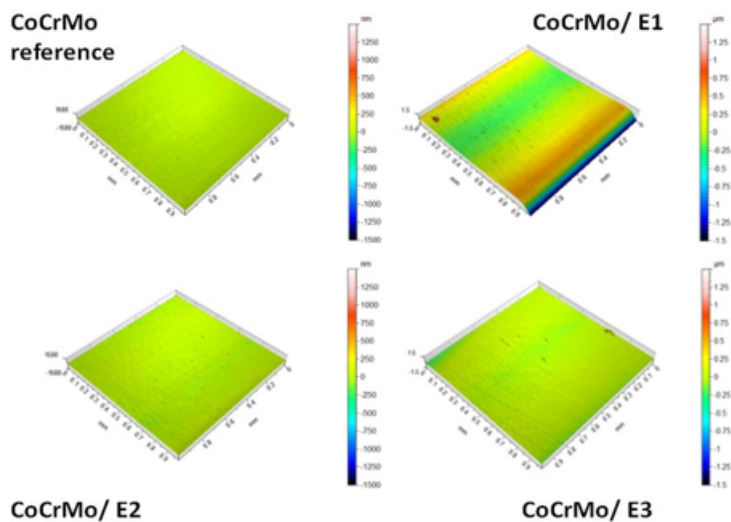


Fig. 7. 3D image of CoCrMo topography

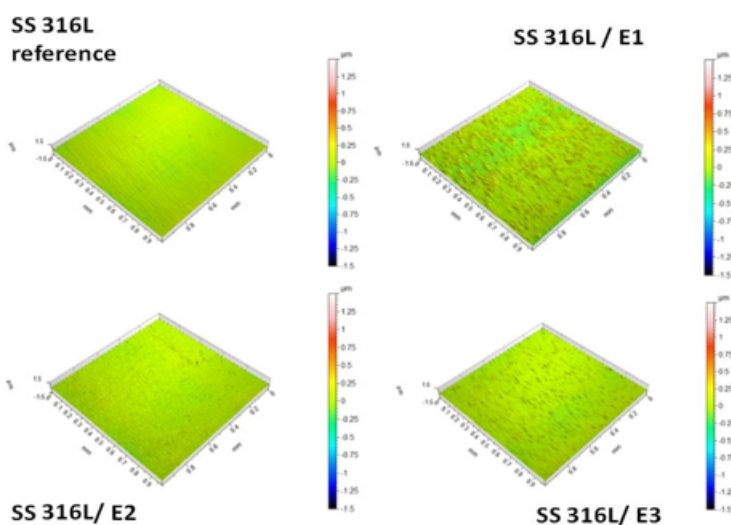


Fig. 8. 3D image of SS 316L topography

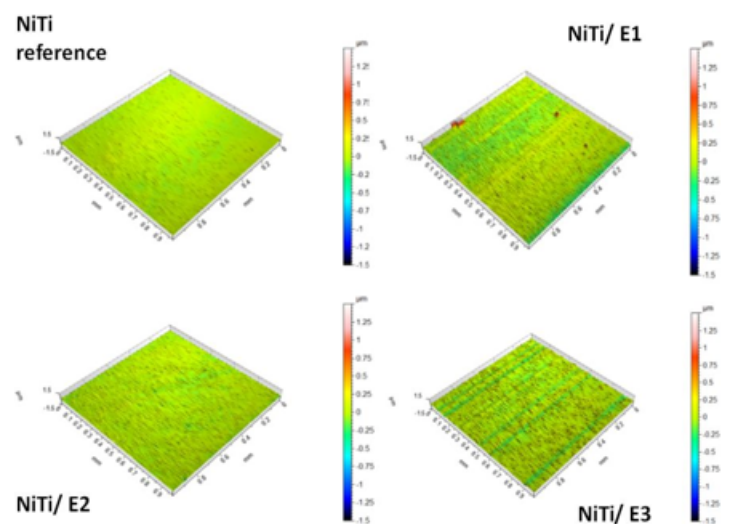


Fig. 9. 3D image of NiTi topography

Table 8
THE MEASUREMENTS FOR ROUGHNESS ACCORDING TO ISO 25178

Sample	Roughness (nm)
CoCrMo reference	11.3
CoCrMo/ E1	24.7
CoCrMo/ E2	22.2
CoCrMo/ E3	17.9
SS 316L reference	29.2
SS 316L/ E1	23.9
SS 316L/ E2	67.3
SS 316L/ E3	26.7
NiTi reference	31.5
NiTi/ E1	82.1
NiTi/ E2	38.3
NiTi/ E3	77.5

SS 316L alloy indicates high roughness in the saliva with the addition of 0.1% NaF, which can be explained by the existence of the second protective layer at the surface, fact evidenced by EIS spectra as well. In case of NiTi alloy, all the samples immersed for 10 days exhibit high values of the roughness compared to reference.

Conclusions

Three different materials used in dentistry were tested in artificial saliva and modified saliva with addition of sodium fluoride. The influence of fluoride was investigated for a period of ten days with electrochemical measurements and topography analysis. The best electrochemical behavior with a good corrosion resistance

was found for the CoCrMo alloy, followed by stainless steel alloy. NiTi alloy was the most affected by the addition of fluoride and the corrosion rate increased dramatically. Based on our experimental data we can conclude that the addition of sodium fluoride increase the corrosion rate. The electrochemical impedance spectroscopy indicated a phase angle close to -80° maintained in a wide domain of frequencies, denoting the presence of a thin passive oxide film on the surface of materials. The topography and the roughness measurements have shown the highest values for CoCrMo and NiTi alloys.

Acknowledgements: The work has been funded by the Sectoral Operational Programme Human Resources Development 2007-2013 of the Ministry of European Funds through the Financial Agreement POSDRU/159/1.5/S/134398. The financial support enabled the stay of D.C.R. at the Jožef Stefan Institute. The work was carried out within the grant No. P2-0393 financed by the Slovenian Research Agency.

References

1. MAN, I., PIRVU, C., DEMETRESCU, I., Rev. Chim. (Bucharest), **59**, no. 6, 2008, p. 615.
2. GOLGOVICI, F., PRODANA, M., POPESCU, A., Rev. Chim. (Bucharest), **66**, no. 5, 2015, p. 660.
3. IONITA, D., MAN, I., DEMETRESCU, I., Key Engineering Mater, **330-332**, 2007, p. 545.
4. TOTEA, G., BRANZOI, I.V., IONITA, D., Rev. Chim. (Bucharest), **64**, no. 6, 2013, p. 625.
5. ELSHAHAWY, W., WATANABE, I., Tanta Dental Journal, **11**, 2014, p. 150.
6. MISCH, C. E., Contemporary Implant Dentistry, Mosby-Year Book, Inc., 1993, ISBN: 08016-6073-4, p. 259.
7. THOMPSON, S. A., Blackwell Science, Ltd REVIEW An overview of nickel-titanium alloys used in dentistry, International Endodontic Journal, **33**, 2000, p. 297.
8. RADEV, D.D., ISRN Metallurgy, Article ID 464089, 6 pages, 2012. doi:10.5402/2012/464089
9. MILOŠEV, I., STREHBLOW, H.H., Electrochim. Acta, **48**, 2003, p. 2767.
10. WEVER, D.J., VELDHIJZEN, A.G., de VRIEWS, J., BUSSCHER, H.J., UGES, D.R., van HORN. J.R., Biomaterials, **19**, 1998, p. 761.
11. GRANCHI, D., CIAPETTI, G., SAVARINO, L., STEA, S., FILIPPINI, F., SUDANESE, A., ROTINI, R., GIUNTI, A., Biomaterials, **21**, 2000, p. 2059.
12. METIKOS-HUKOVIÆ, M., KATIÆ, J., MILOŠEV, I., J. Solid State Electrochem., **16**, 2012, p. 2503
13. MILOSEV, I., KAPUN, B., Mat. Sci. Eng. C, **32**, nr. 5, 2012, p. 1068.
14. MILOSEV, I., KAPUN, B., Mat. Sci. Eng. C, **32**, nr. 5, 2012, p. 1087.
15. MILOSEV, I., KAPUN, B., ŠELIH, V.S., Acta Chim. Slov., **60**, 2013, p. 543.
16. DIAMANTI, I., KOLETZI-KOUNARI, H., MAMAI-HOMATA, E., VOUGIOUKLAKIS, G., J. of Dentistry, **39**, nr. 9, 2011, p. 619.
17. GRIFFIN, S.O., REGNIER, E., GRIFFIN, P.M., HUNTLEY, V., J. Dent. Res., **86** nr. 5, 2007, p. 410.
18. IONITA, D., PRODANA M., DEMETRESCU I., STANCIU, S.G., STANCIU, G.A., Mat. Corr., **12**, 2011, p. 1111.
19. DUFFO, G. S., QUEZADA CASTILLO, E., Corrosion, **60**, 2004, p. 594.

Manuscript received: 24.09.2015